

NUMERICAL SIMULATION OF THE STRATIFIED FLOW USING HIGH ORDER SCHEMES

Luděk Beneš*, Jiří Fůrst*, Philippe Fraunie**

The article deals with the numerical simulation of unstable, incompressible flows with stratifications. The mathematical model is based on the Boussinesq approximation of the Navier-Stokes equations. The flow field in the towing tank with a moving cylinder is modeled for wide range of Richardson numbers. The obstacle is modeled via appropriate source terms. The resulting set of PDE is then solved by the fifth order WENO scheme, or by a second order finite volume AUSM MUSCL scheme. Both schemes are combined with the artificial compressibility method in dual time.

Keywords: stratified flow, towing tank, Boussinesq approximation, finite volume, WENO artificial compressibility

1. Boussinesq approximation

Flows in the atmosphere are characterized by relatively small velocities. It allows us to consider them as incompressible ($\nabla \cdot \vec{u} = 0$). Nevertheless, their density isn't constant due to different temperature, gravity etc. Therefore the equation for the density has to be considered. The Navier-Stokes equations describing such flows are

$$\frac{D\rho}{Dt} = 0, \quad (1)$$

$$\rho \frac{D\vec{u}}{Dt} = -\nabla p + \mu \Delta \vec{u} + \rho \vec{g} + \vec{f}. \quad (2)$$

Here ρ is the density, $\vec{u} = (u, v, w)$ is the velocity, p is the pressure, μ is the dynamic viscosity, $\vec{g} = (0, 0, -g)$ is the gravity, and \vec{f} are other forces (e.g. Coriolis force).

These equations are simplified by Boussinesq approximation. Density and pressure are divided into two parts – background part + perturbation

$$\rho = \rho_0(z) + \rho'(x, y, z, t), \quad (3)$$

$$p = p_0(z) + p'(x, y, z, t). \quad (4)$$

Background part is chosen to fulfill hydrostatic balance $\partial p_0(z)/\partial z = -\rho_0(z)g$. Appearing system of equations is partly linearized around the average state ρ_* . Resulting set of equations can be written in the next form

$$\frac{D\rho'}{Dt} = -w \frac{d\rho_0}{dz}, \quad (5)$$

* Ing. L. Beneš, Ph.D., doc. Ing. J. Fůrst, Ph.D., Department of Technical Mathematical, Faculty of Mechanical Engineering, CTU Prague, Karovo nám. 13, 121 35 Prague, Czech Republic

** prof. P. Fraunie, LSEET/CNRS Université de Toulon et du Var, France

$$\frac{D\vec{u}}{Dt} + \frac{1}{\rho_*} \nabla p' = \nu \Delta \vec{u} + \frac{\rho'}{\rho_*} \vec{g} + \frac{1}{\rho_*} \vec{f}, \quad (6)$$

$$\nabla \vec{u} = 0. \quad (7)$$

For the description of the stratification effects, the bulk Richardson number of the following form

$$Ri = \frac{g L \frac{\partial \rho_0}{\partial z}}{\rho_* U^2} \quad (8)$$

was introduced. Here L is characteristic length and U characteristic velocity. This non-dimensional parameter follow directly from the non-dimensional form of the Boussinesque equations as the parameter associated with gravity force.

We will assume $\rho_* = 1$ and we will drop the primes above density and pressure disturbances.

2. Artificial compressibility method

The equations (5)–(7) are rewritten in the conservative form. The equations in 2D are (y is the vertical coordinate and v is the velocity component parallel to gravity force in the following text)

$$P W_t + F(W)_x + G(W)_y = S(W).$$

Here $W = [\rho, u, v, p]^T$, $F = F^i - \nu F^v$ and $G = G^i - \nu G^v$ contain the inviscid fluxes F^i , G^i and viscous fluxes F^v and G^v , S is the source term, and $P = \text{diag}(1, 1, 1, 0)$. The numerical solution is achieved using the artificial compressibility method in dual time, hence the steady state solution (with resp. to artificial time τ) of

$$\tilde{P} W_\tau + P W_t + F(W)_x + G(W)_y = S(W), \quad (9)$$

is computed in each physical time step. The matrix \tilde{P} is given as $\tilde{P} = \text{diag}(1, 1, 1, 1)$ and the fluxes and the source term are

$$\begin{aligned} F^i(W) &= [\rho u, u^2 + p, u v, \beta^2 u]^T, & G^i(W) &= [\rho v, u v, v^2 + p, \beta^2 v]^T, \\ F^v(W) &= [0, u_x, v_x, 0]^T, & G^v(W) &= [0, u_y, v_y, 0]^T, \\ S(W) &= [-v d\rho_0/dz, 0, -\rho g, 0]^T. \end{aligned} \quad (10)$$

3. Numerical schemes

Two different numerical schemes were used for the spatial semidiscretization. The first scheme is based on a flux splitting method and WENO interpolation. The second one were the AUSM MUSCL scheme with Hemker–Koren limiter.

3.1. Flux splitting for incompressible flows

The discretization in space dimensions are achieved by standard fourth order differences for viscous terms and by the following high order flux-splitting method.

The inviscid flux $F^i(W)$ is divided onto two parts, the convective flux $F^c(W) = [\rho u, u^2, u v, 0]^T$ and pressure flux $F^p(W) = [0, p, 0, \beta^2 u]^T$. The derivative F_x is then approximated as

$$F^i(W)_x|_i \approx \frac{1}{\Delta x} [F_{i+1/2}^c - F_{i-1/2}^c] + \frac{1}{\Delta x} [F_{i+1/2}^p - F_{i-1/2}^p]. \quad (11)$$

The high order weighted ENO scheme [1] is chosen as the interpolation method. The original WENO interpolation uses an upwind bias and it can be formally written in the following form (function `weno5` is described in [2]):

$$\phi_{i+1/2} = \begin{cases} \phi_{i+1/2}^+ = \text{weno5}(\phi_{i-2}, \phi_{i-1}, \phi_i, \phi_{i+1}, \phi_{i+2}) & \text{if } u_{i+1/2} > 0, \\ \phi_{i+1/2}^- = \text{weno5}(\phi_{i+3}, \phi_{i+2}, \phi_{i+1}, \phi_i, \phi_{i-1}) & \text{if } u_{i+1/2} \leq 0. \end{cases} \quad (12)$$

It is still necessary to determine the velocity $u_{i+1/2}$.

This interpolation is applied to incompressible case separately for convective and pressure terms. Eigenvalues of Jacobi matrix of convective part are $\lambda_1 = 0$, $\lambda_{2,3} = u$, $\lambda_4 = 2u$. Eigenvalues of Jacobi matrix of pressure part are $\lambda_{1,2} = 0$, $\lambda_{3,4} = \pm\beta$ and characteristic variables $[\rho, v, (\beta u + p)/(2\beta), (\beta u - p)/(2\beta)]^T$. According to this analysis, the convective part is discretized by simple upwind, the third component of pressure part is approximated by backward difference and the fourth component by forward difference. Finally, the scheme takes next form

$$u_{i+1/2} := (u_{i+1/2}^+ + u_{i+1/2}^-)/2, \quad p_{i+1/2} := (p_{i+1/2}^+ + p_{i+1/2}^-)/2, \quad (13)$$

$$F^c(W)_{i+1/2} := \begin{bmatrix} (\rho u)_{i+1/2}^\pm \\ (u^2)_{i+1/2}^\pm \\ (u v)_{i+1/2}^\pm \\ 0 \end{bmatrix}, \quad F^p(W) := \begin{bmatrix} 0 \\ p_{i+1/2} + \beta \frac{u_{i+1/2}^+ - u_{i+1/2}^-}{2} \\ 0 \\ u_{i+1/2} + \frac{p_{i+1/2}^+ - p_{i+1/2}^-}{2\beta} \end{bmatrix}, \quad (14)$$

where + or - is taken in the convective flux according to the sign of $u_{i+1/2}$.

Similar algorithm is applied in y direction for the flux G . The resulting scheme poses high order of accuracy in space. Referred scheme was validated through computation of shock-vortex interaction, see [5] and by comparison with different schemes see [3].

3.2. AUSM scheme

In the second scheme, the finite volume AUSM scheme was used for spatial discretization of the inviscid fluxes:

$$\int_{\Omega} (F_x^i + G_y^i) dS = \oint_{\partial\Omega} (F^i n_x + G^i n_y) dl \approx \sum_{k=1}^4 \left[u_n \begin{pmatrix} \rho \\ u \\ v \\ \beta^2 \end{pmatrix}_{L/R} + p \begin{pmatrix} 0 \\ n_x \\ n_y \\ 0 \end{pmatrix} \right] \Delta l_k \quad (15)$$

where n is normal vector, u_n is normal velocity vector, and $(q)_{L/R}$ are quantities on left/right hand side of the face. These quantities are computed using MUSCL reconstruction with Hemker-Koren limiter.

$$q_R = q_{i+1} - \frac{1}{2}\delta_R, \quad q_L = q_i + \frac{1}{2}\delta_L, \quad \delta_{L/R} = \frac{a_{L/R}(b_{L/R}^2 + 2) + b_{L/R}(2a_{L/R}^2 + 1)}{2a_{L/R}^2 + 2b_{L/R}^2 - a_{L/R}b_{L/R} + 3},$$

$$a_R = q_{i+2} - q_{i+1} \quad a_L = q_{i+1} - q_i, \quad b_R = q_{i+1} - q_i, \quad b_L = q_i - q_{i-1}.$$

Because of the pressure is discretized by central way, the scheme is stabilized by the pressure diffusion

$$F_{\mathbf{d}i+1/2,j} = \begin{pmatrix} 0 \\ 0 \\ 0 \\ \eta \frac{p^{i+1,j} - p_{i,j}}{\beta_x} \end{pmatrix}, \quad \beta_x = w_r + \frac{2\nu}{\Delta x}$$

where w_r is reference velocity (in our case the maximum velocity in flow field).

Viscous fluxes are discretized in central way on dual mesh. This scheme is of the second order accuracy in space.

3.3. Time integration

The derivative with respect to the physical time t is discretized either by the second order BDF formula,

$$\begin{aligned} P \frac{3W^{n+1} - 4W^n + W^{n-1}}{2\Delta t} + F_x^{n+1}(W) + G_y^{n+1}(W) &= S^{n+1}, \\ Rez^{n+1}(W) = P \left(\frac{3}{2\Delta t} W^{n+1} - \frac{2}{\Delta t} W^n + \frac{1}{2\Delta t} W^{n-1} \right) + & \\ + F_x^{n+1}(W) + G_y^{n+1}(W) - f^{n+1} - S^{n+1}. & \end{aligned} \quad (16)$$

Arising system of equations

$$Rez^{n+1}(W) = 0$$

is solved by artificial compressibility method in the dual time τ by an explicit 3-stage Runge-Kutta method.

Both schemes are of the second order in time.

4. Obstacle modeling

We are interested in the solution of the stratified flows in a towing tank with spherical obstacle. The obstacle is modeled using very simple source term emulating a porous media with small permeability. The source term S would be in this case

$$S(W) = \left[-v \frac{d\rho_0}{dz}, 0, -\rho g, 0 \right]^T + \frac{\chi(x, y, t)}{K} [0, U^{\text{ob}} - u, V^{\text{ob}} - v, 0]^T, \quad (17)$$

where K corresponds to small permeability, $\chi(x, y, t)$ is the characteristic function of the obstacle moving with the velocity $(U^{\text{ob}}, V^{\text{ob}})$.

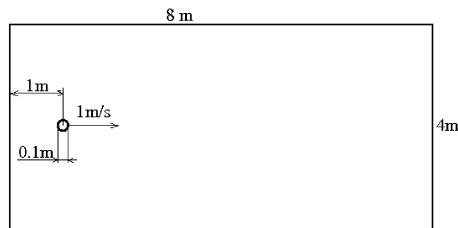


Fig.1: Towing tank

5. Numerical results

The towing tank (see fig. 1) is a 2D channel with the dimensions 8×4 meters with homogeneous Dirichlet boundary conditions for velocity and Neumann conditions for density and pressure disturbances. The flow field is initially at rest with the stable density gradient $d\rho_0/dz = -0.1 \text{ kg/m}^4$. The average density is $\rho_* = 1 \text{ kg/m}^3$ and the kinematic viscosity is $\nu = 10^{-4} \text{ m}^2/\text{s}$. The obstacle is located 1m from the left wall in the middle height.

The obstacle is a cylinder with radius $L = 0.1 \text{ m}$, and in the time $t = 0$ the obstacle starts moving to the right with a constant velocity $U = U^{\text{ob}} = 1 \text{ m/s}$. The permeability was chosen $K^{-1} = 10 \text{ s}^{-1}$.

The problem was solved on a Cartesian mesh with 320×160 nodes and, for testing of mesh independence, on the fine grid with 640×320 nodes.

Various level of the stratification was modeled. The degree of the stratification isn't changed by the changing of density gradient, but by the modification of the gravity constant in the range $g \in (0, 1000)$. Corresponding Richardson numbers varies in $Ri \in (0, 100)$. Both numerical methods were compared.

The figures 2–4 show comparison of both schemes. The first picture shows the comparison of density isolines in given time $t = 5 \text{ s}$. On the next two figures is displayed comparison of

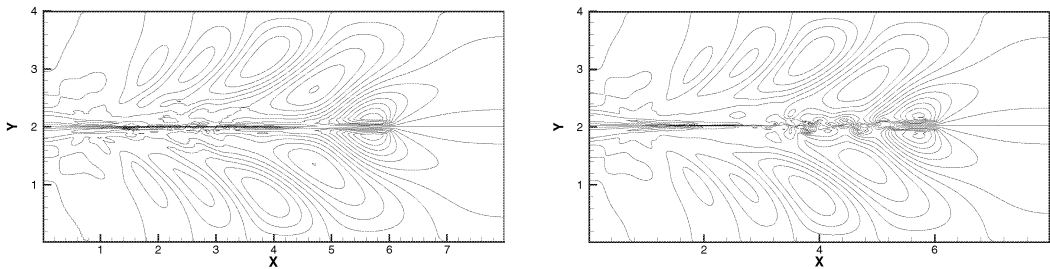


Fig.2: Comparison of isolines of the density disturbances for towing tank problem at the time $t = 5 \text{ s}$, $g = 100$, $Ri = 10$; AUSM MUSCL scheme left and WENO5 right

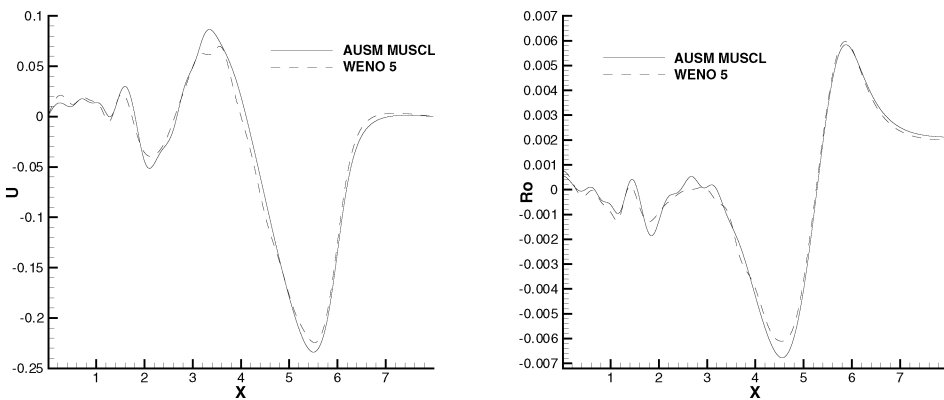


Fig.3: Comparison of both schemes, $Ri = 10$, $g = 100$, time $t = 5 \text{ s}$; longitudinal distribution of the u -velocity component (left) and density disturbances (right), $y = 2.25$

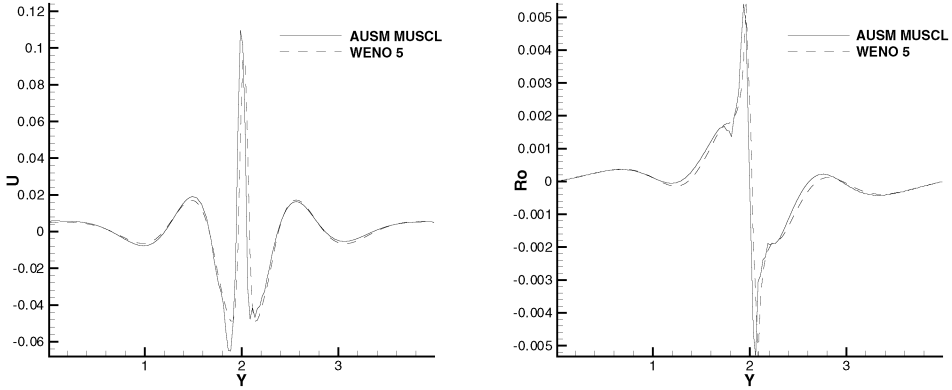


Fig.4: Comparison of both schemes, $Ri = 10$, $g = 100$, time $t = 5$ s; transversal distribution of the u -velocity component (left) and density disturbances (right), $x = 1$

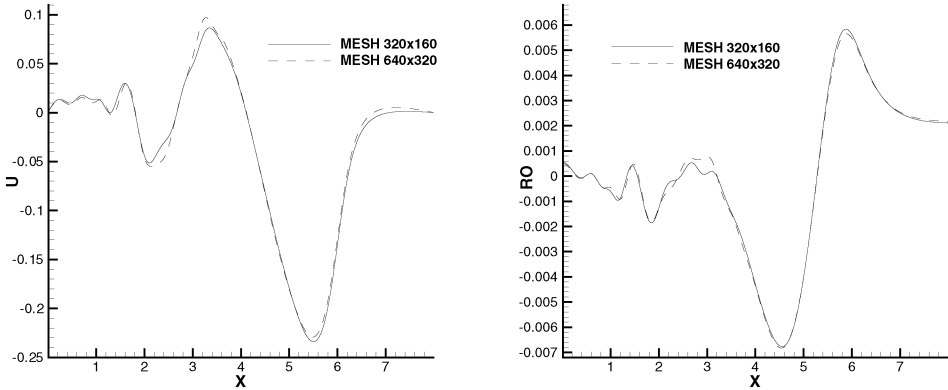


Fig.5: Dependence on the mesh, AUSM MUSCL scheme, $Ri = 10$, $g = 100$, time $t = 5$ s; longitudinal distribution of the u -velocity component (left) and density disturbances (right), $y = 2.25$

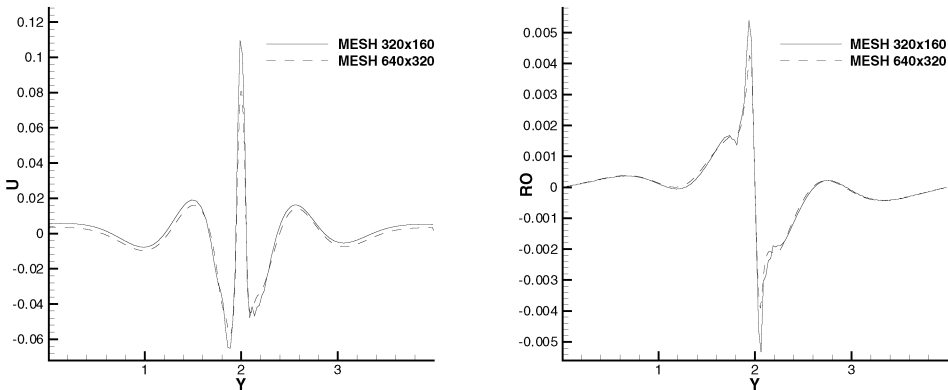


Fig.6: Dependence on the mesh, AUSM MUSCL scheme, $Ri = 10$, $g = 100$, time $t = 5$ s; transversal distribution of the u -velocity component (left) and density disturbances (right), $x = 1$

distribution of selected quantities in transversal and longitudinal directions. On figs. 2–4 we can see good agreement both methods. Only maximal values predicted by WENO 5 scheme in the middle height are rather lower.

The next two figures (figs. 5, 6) show dependency on the mesh for the AUSM MUSCL scheme. From this one can see, that solution is relatively mesh independent. Only maxima of quantities in the middle height are lower and probably they aren't correctly resolved on coarse mesh.

On figures 7, 8 we can see development of the flow for two different Richardson numbers. For the lower level of stratification behind the obstacle Karman vortex street forms. When the level of stratification increase, the character of the flow is changing. Turbulent mixing is damped by the stratification, internal gravity waves are clearly visible. Behind the obstacle generates strip with constant density (see also [4], [6]). On the figure 9 was displayed transversal and longitudinal distribution of the computed quantities in the case of AUSM MUSCL scheme. The changing of the character of the flow and the wave character of the flow is well shown.

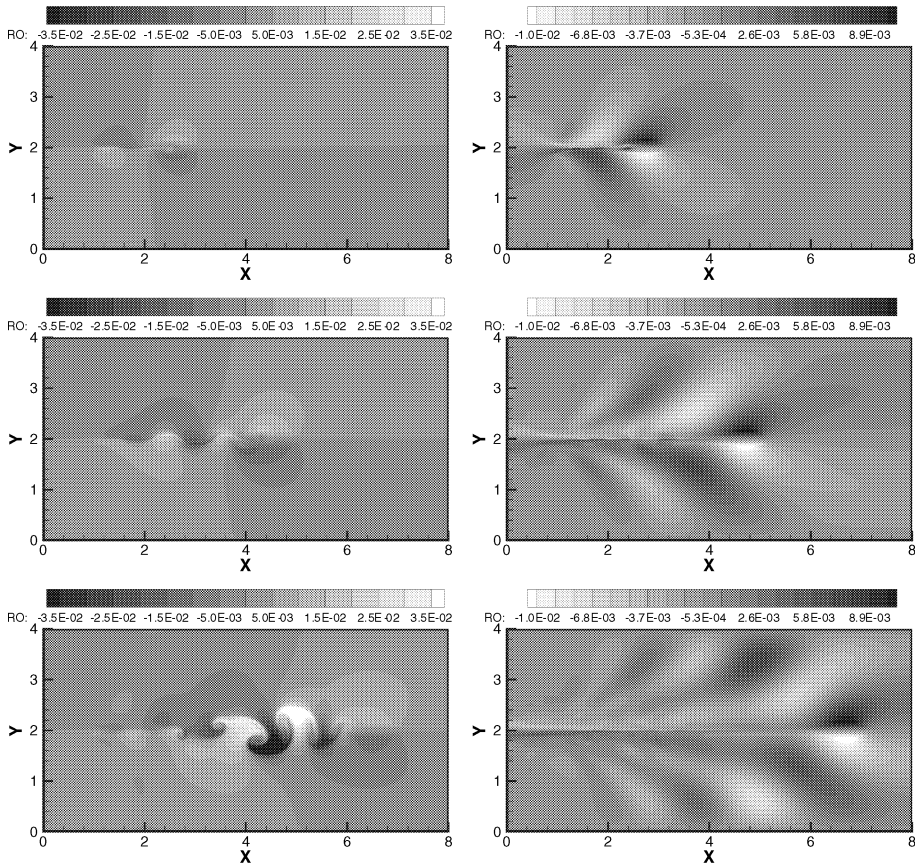


Fig.7: Isolines of the density disturbances for two different Richardson numbers, $Ri = 1$, $g = 10$ (left), $Ri = 10$, $g = 100$ (right), at the times $t = 2, 4, 6$ s AUSM MUSCL

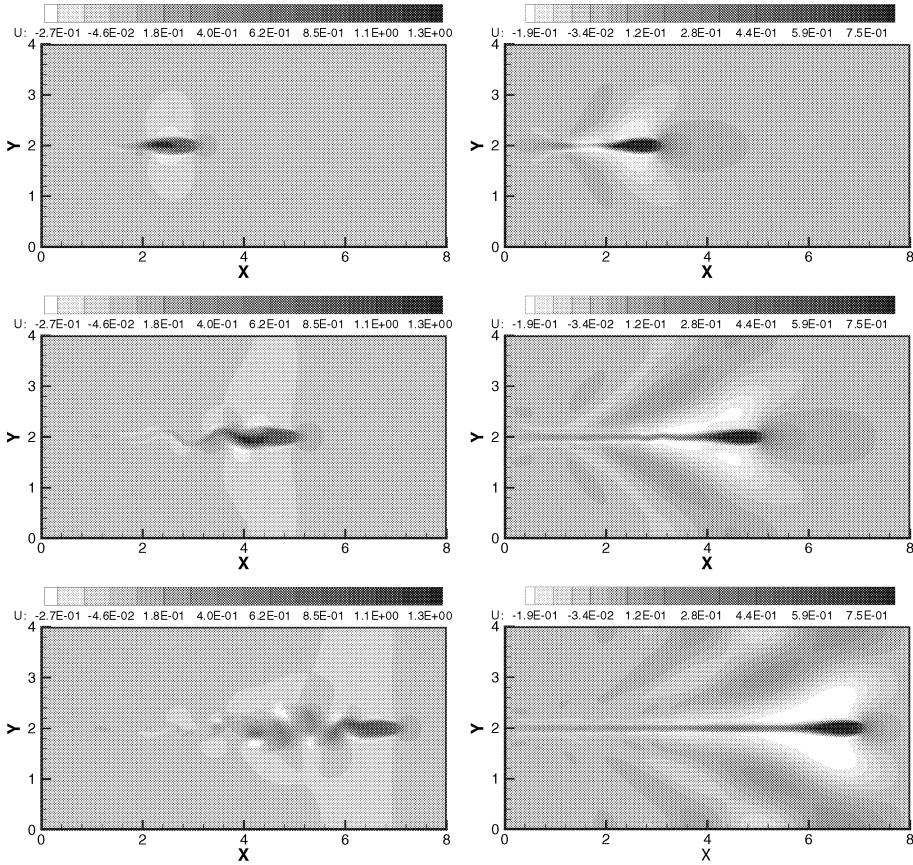


Fig.8: Isolines of the u -velocity component for two different Richardson numbers, $Ri = 1$, $g = 10$ (left), $Ri = 10$, $g = 100$ (right), at the times $t = 2, 4, 6$ s AUSM MUSCL

6. Conclusion

Two numerical schemes for stratified flows have been developed and they have been used successfully for towing tank problem. Several numerical results for different Richardson numbers were obtained. The performed computations show a good applicability of our methods to simulations of stratified flows. The results obtained using these schemes are in good agreement each other. These results also correspond to linear theory of gravity waves (see fig. 9).

On the other hand, there are some open questions. One of them is the influence of permeability parameter on the flow behind the obstacle. Other question is the choice of the boundary conditions. The conditions used in the current approach are suitable for the simulation of the flows in a bounded domain with walls. Another kind of conditions should be considered for the flows in free atmosphere.

Acknowledgments

The work was supported by the Research Plans MSM 6840770003 and MSM 6840770010 and by the project of the GACR No. 205/06/0727.

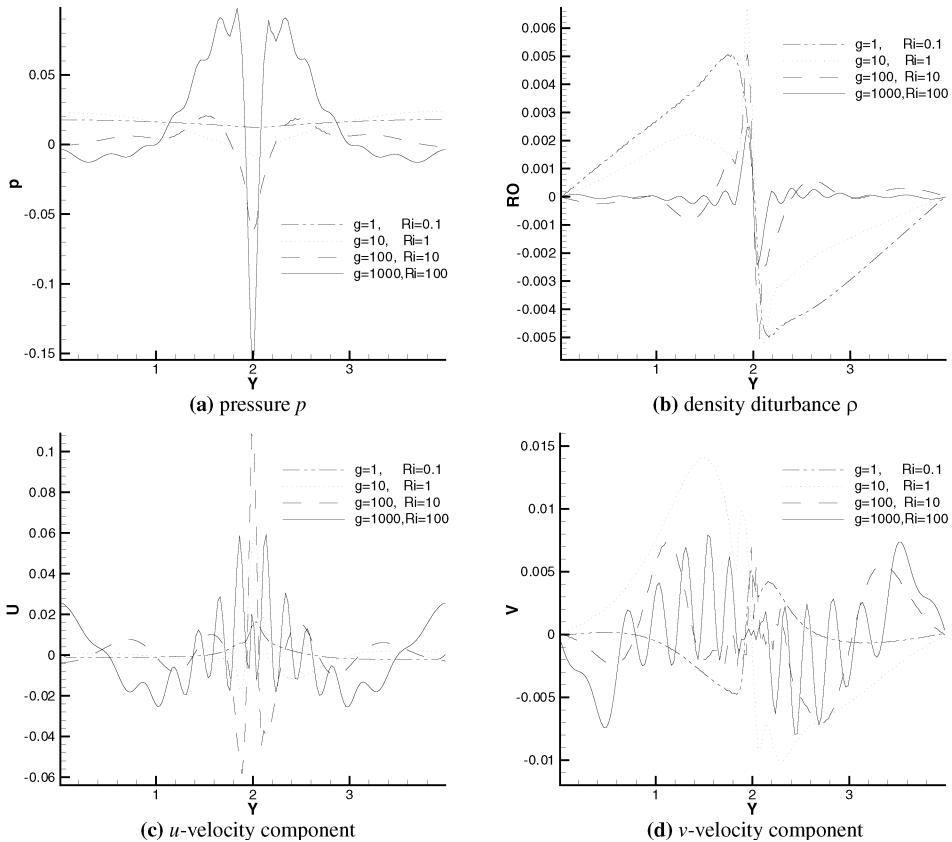


Fig.9: Transversal distribution of computed quantities for different Richardson numbers, AUSM MUSCL scheme, $x = 1$, time $t = 6$ s

References

- [1] Issa R.I.: Solution of the implicitly discretized fluid flow equations by operator-splitting, *Journal of Computational Physics*, 62:40–65, 1985
- [2] Jiang G.-S., Shu Ch.-W.: Efficient implementation of weighted ENO schemes, *Journal of Computational Physics*, 126:202–228, 1996
- [3] Fürst J., Fraunie P.: The High Order Schemes for Stratified Flows, *Proceeding of conference Topical Problems of Fluid Mechanics 2007*, p. 49–52, ISBN 978-80-87012-04-8
- [4] Beneš L., Fürst J., Fraunie P.: Numerical Simulation of the Stratified Flow, *Proceeding of conference Topical Problems of Fluid Mechanics 2008*, p. 5–8, ISBN 978-80-87012-09-3
- [5] Angot P., Fürst J., Kozel K.: TVD and ENO Schemes for Multidimensional Steady and Unsteady Flows, *Finite Volumes for Complex Applications*, pp. 283–290, Hermes 1996, ISBN 2-86601-556-8
- [6] Berrabaa S., Fraunie P., Crochet M.: 2D Large Eddy Simulation of Highly Stratified Flow: The Stepwise Structure Effect, *Advances in Computation: Theory and Practice Vol. 7*, pp. 179–185, Nova Science Publishers 2001, ISBN 1-59033-027-7

Received in editor's office: June 4, 2008

Approved for publishing: September 24, 2008

Note: The paper is an extended version of the contribution presented at the conference *Topical Problems of Fluid Dynamics 2008, Prague, 2008*.